15499 VITROPHYRIC QUARTZ-NORMATIVE MARE BASALT ST. 4 2024 g

INTRODUCTION: 15499 is a vitrophyric pigeonite basalt collected from the top of the same vesicular boulder on the south rim of Dune Crater as the similar samples 15485 and 15486 (Fig. 1). It is one of the most-rapidly cooled of the quartz-normative basalts and has an age of ~3.3 b.y.

15499 is a vesicular basalt with a porphyritic, diktytaxitic texture (Fig. 2). It is medium-dark gray, blocky and angular, and tough. It was broken from the boulder, hence has a fresh surface, and the other side has zap pits.

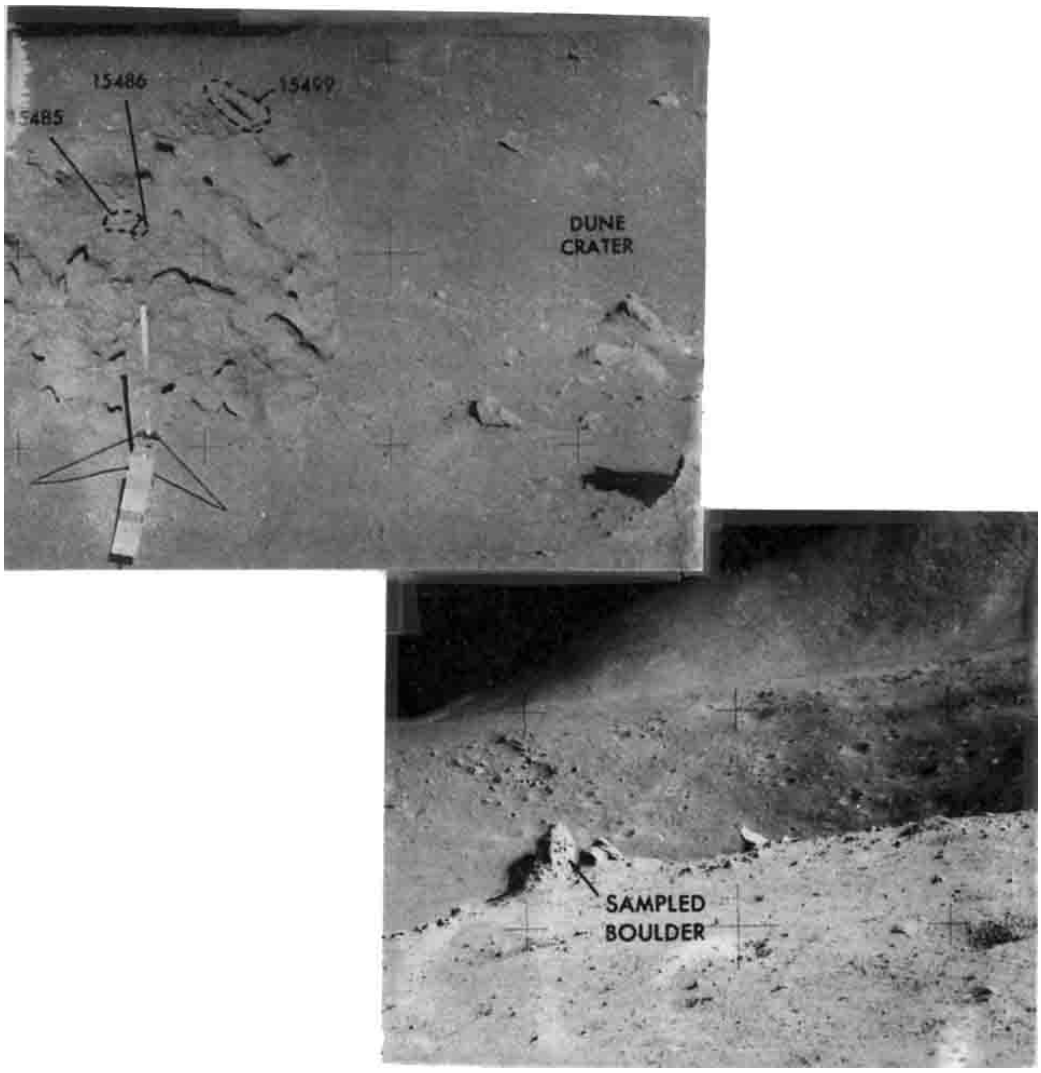

Figure 1. Sampling locations for 15485, 15486, and 15499 from a boulder on the south rim of Dune Crater.

PETROLOGY: 15499 contains abundant euhedral pyroxene phenocrysts, with yellowish cores and brown rims, up to 1 cm long, set in a dark brownish gray groundmass (Fig. 3). A general description of thin section ,4 was given in the Apollo 15 Lunar Sample Information Catalog, which stated that the sample is porphyritic (42%) with a fine-grained groundmass (>57%). The groundmass contains clinopyroxene (52% of rock), 5% ilmenite, and minor Fe-Ni metal, Cr-spinel, troilite, and ulvospinel. Rhodes and Hubbard (1973) reported a similar mode for ,7: 41.8% pyroxene, 0.8% olivine, and 57.3% groundmass, with the same identified trace minerals. Bence and Papike (1972) also noted the single large skeletal olivine phenocryst: it is extremely zoned from an Fo_{88} core to an Fo_{88} rim. Brief general descriptions of the rock are also given by Papike et al. (1972) and Bence and Papike (1972). The crystallization sequence of olivine→olivine + pigeonite→pigeonite + augite→augite + plagioclase (Bence and Papike 1972) is an agreement with the experimental results (below). Very little olivine developed. The pyroxenes are composite with pigeonite core and augite rims. The groundmass is a variolitic aggregate of coprecipitating plagioclase, augite, and glass. Oxide phases occur only in the groundmass. Several studies have focused on determining the cooling history of 15499.

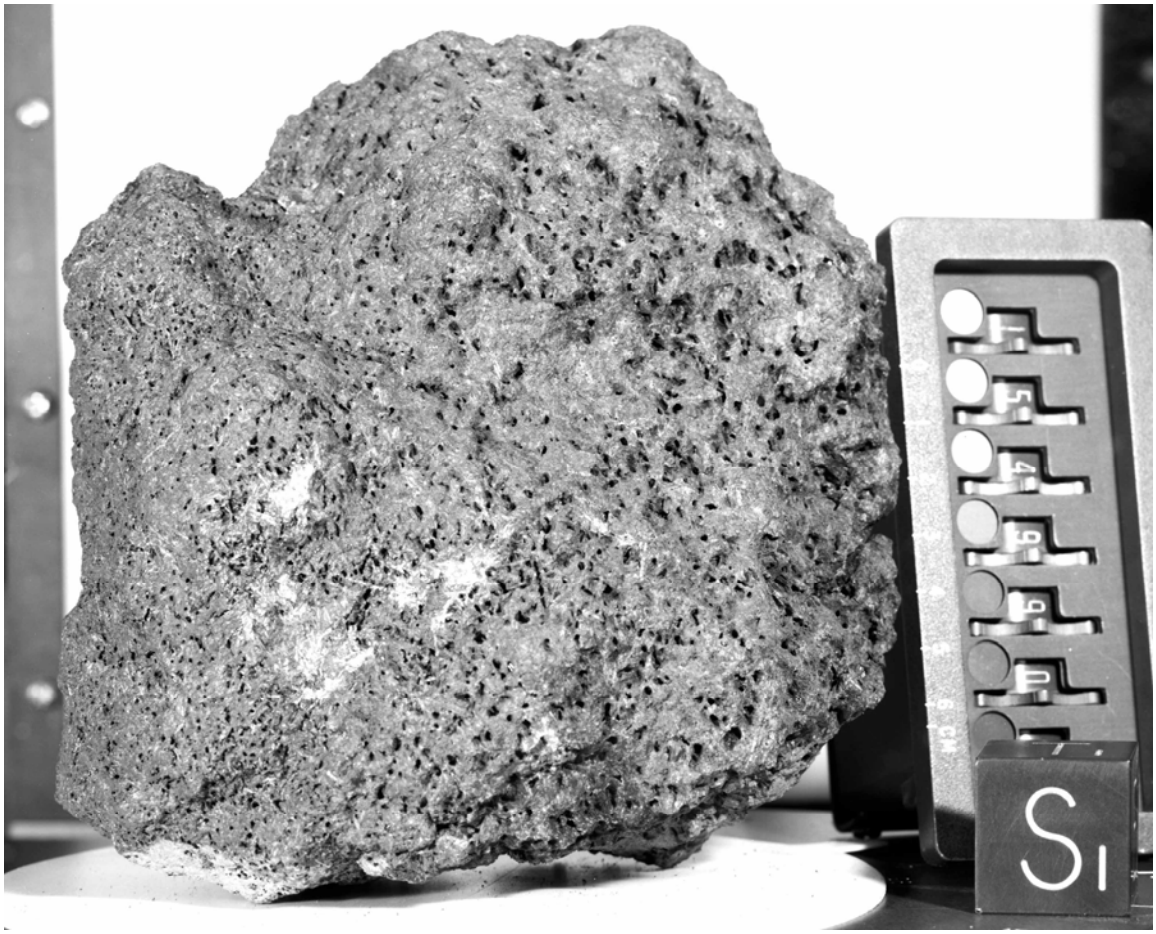

Fig. 2a

Fig. 2b

Figure 2. Macroscopic views of 15499 prior to any chipping, showing angular, tabular nature, and diktytaxitic texture. S-71-47704 and S-71-47690.

The pyroxenes are described by Papike et al. (1972), Bence and Papike (1972), Bence and Autier (1972), and Grove and Walker (1977). Compositional variations are shown in Figure 4. Papike et al. (1972) studied exsolution relationships using single crystal x-ray

diffraction and microprobe techniques, and found virtually no exsolution. They noted that the phenocrysts are well developed with little evidence for resorption, consistent with a rapid, late-stage quench. The phenocrysts show a continuous buildup of Al to nearly 10% Al_2O_3 in augite rims (Bence and Papike 1972), and there is no Ca-discontinuity, consistent with the interpretation that plagioclase did not precipitate until the phenocrysts to all intents and purposes stopped growing. The phenocrysts show two crystallization trends, according to growing direction. Pyroxene analyses are tabulated by Bence and Papike (1972) (Table 1). Bence and Autier (1972) used secondary ion mass analysis and the electron microprobe to analyze for several minor elements along traverses (Fig. 5). Abu-Eid et al. (1973) studied electronic absorption and Mossbauer spectra for a hand-picked pyroxene, finding significant Ti^{3+} in the rims of pyroxenes, and that Fe^{3+} was below their 1% detectability limit.

E1 Goresy et al. (1976) studied zoning in the spinels, noting that 15499 and other fine-grained quartz-normative basalts have spinels with chromite cores which display idiomorphic sharp boundaries to an ulvospinel rim, without a sign of reaction prior to ulvospinel precipitation (in contrast with the corroded cores in coarse basalts). No details are presented for 15499 specifically, although the authors state that a number of spinels in 15499 were analyzed. Engelhardt (1977) tabulates ilmenite paragenesis.

Cooling history: Several petrological studies have been directed at establishing the cooling history of 15499, mainly from a comparison of the rock with products of dynamic crystallization experiments on a similar composition. Lofgren et al. (1974) found that the morphology and zoning of 15499 phenocrysts resembled those in experiments conducted with linear cooling rates of 1.2°C to 30°C/hr, and a comparison of the core compositions suggests that the nucleation was at 1190°C i.e., supercooled 30°C. The results do not require a two-stage cooling history. A further study (Lofgren et al., 1975) of phenocryst shapes and matrix textures indicated 5-20°C/hr and 10-30°C/hr respectively, and 15499 to be one of the fastest-cooled quartz-normative basalts. Grove and Walker (1977) made a more detailed study, again using comparisons with dynamic experiments. The pyroxene nucleation density suggests 1.75°C to 3.75°C/hr at nucleation, the phenocrysts size suggests an integrated phenocryst cooling rate of 1.75°C/hr, and the plagioclase sizes suggest a late-stage cooling rate of 30°C/hr., i.e., initial slow cooling and late rapid cooling. A cooling experiment (1°C/hr for 4 days, 30°C/hr for 12 hrs) duplicating these inferred conditions resulted in a very close match with 15499. Both the products of this experiment and 15499 contain skeletal pyroxenes smaller than the phenocrysts but bigger than the groundmass pyroxenes; these are not found in linear cooling rate experiments. Grove and Walker (1977) further concluded that 15499 crystallized ~15 cm from a conductive boundary. In comparison with 15485 and 15486 from the same boulder, 15499 has a similar nucleation density but both pyroxene and plagioclase are coarser. Grove (1982) Studied pyroxenes exsolution with TEM for comparison with experimental analogs. Tweed modulation and heterogeneously-nucleated (001) lamellae are present. On (001) the mean wavelength is 186 Å. Spinodal decomposition is also present on (100). $\Delta\beta$ is 2.67°. The integrated cooling rate estimated from the (001) lamellae wavelength is about 80°C/hr. Brett (1975), using available kinetic data, concluded that 15499 was from a cooling unit ~0.5

m thick. Uhlmann (1981), using a 15499-like composition, studied the characteristics of glass to evaluate the cooling rate, finding that a rate of 14°C/second (much faster than the natural sample) would be required to form a glass.

Fig. 3a

Fig. 3b

Fig. 3c

Figure 3. Photomicrographs of 15499,95.
All transmitted light except (c), crossed polarizers.
(b) and (c) are the same field. All same scale.

EXPERIMENTAL PETROLOGY: Humphries et al. (1972) determined the equilibrium, low pressure crystallization of a 15499 sample, finding results similar to other quartz-normative basalts (Fig. 6): some olivine crystallizes before pyroxene; all olivine reacts out before anorthite entry. They prefer the interpretation that 15499 is a mixture of liquid and accumulated pyroxenes, not a liquid composition.

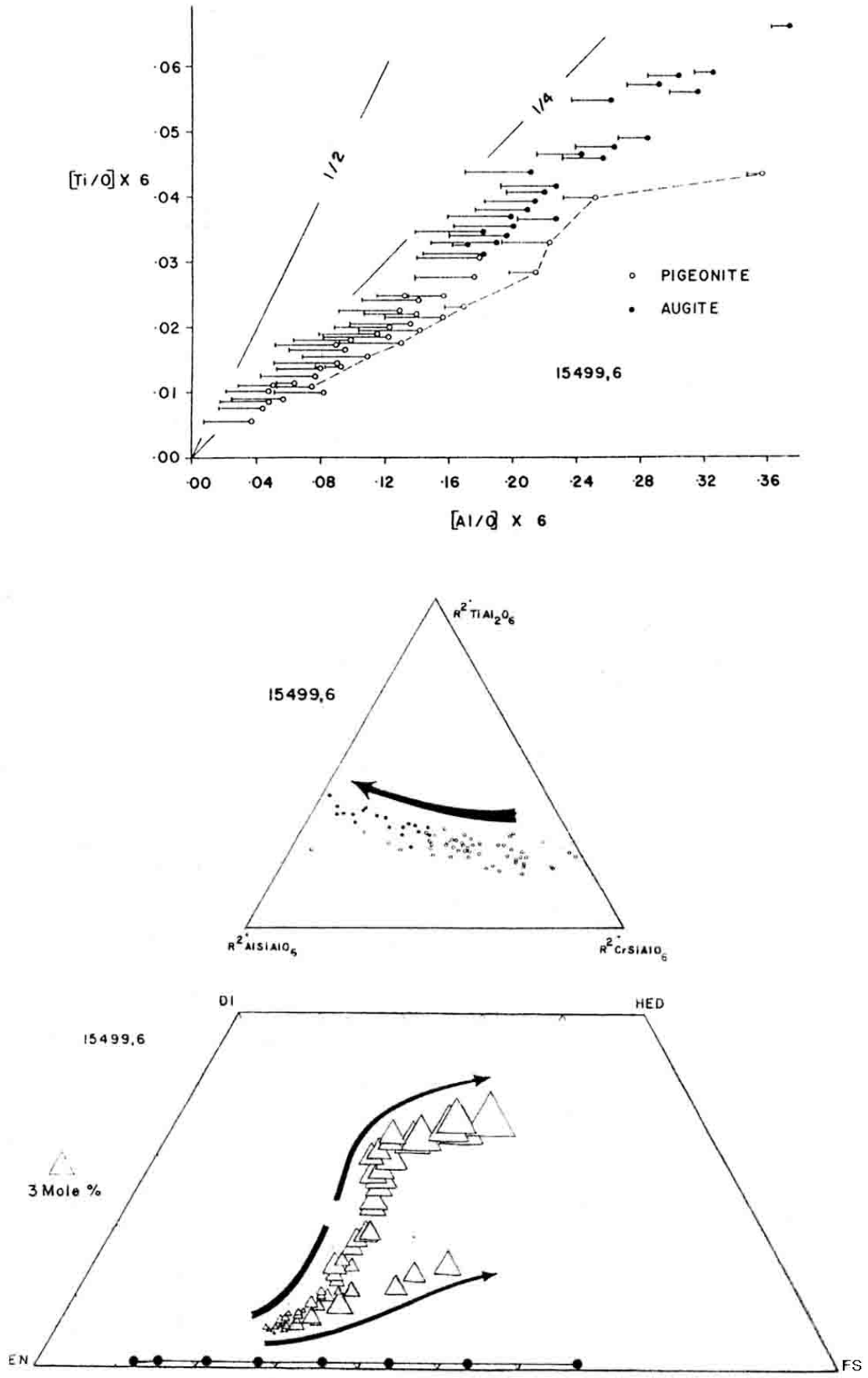

Figure 4. Pyroxene major and minor element plots (Bence and Papike, 1972).

TABLE 15499-1. Representative electron microprobe analyses of pyroxenes from 15499 (Bence and Papike, 1972).

	1	2	3	4	5	6	7	8	9	10	11	12	13	14	15
SiO_2	52.4	52.9	52.1	50.1	50.1	49.4	49.4	49.3	48.5	46.7	43.2	47.8	53.2	52.9	53.2
Al_2O_3	1.89	1.73	1.96	3.55	3.96	4.25	4.35	4.59	5.05	6.67	9.66	4.52	1.75	1.97	1.46
TiO_2	0.36	0.39	0.41	0.88	0.98	1.16	1.30	1.32	1.45	2.01	3.99	0.98	0.43	0.37	0.37
FeO	16.9	17.4	17.5	18.1	18.6	17.5	16.2	16.5	17.4	19.7	20.1	25.0	18.0	16.4	16.5
MgO	23.9	22.6	22.6	18.9	16.5	15.2	14.4	13.1	11.9	9.43	8.58	13.3	21.4	23.1	23.0
CaO	2.62	3.40	3.71	6.51	8.52	10.6	12.2	13.3	14.2	14.3	13.8	6.20	2.96	2.46	2.37
Na_2O	0.03	0.00	0.00	0.00	0.02	0.01	0.05	0.04	0.03	0.02	0.05	0.02	0.00	0.03	0.00
Cr_2O_3	1.04	1.09	1.15	1.18	1.26	1.39	1.45	1.36	1.11	0.71	0.66	0.27	1.08	1.15	1.05
	99.1	**99.5**	**99.4**	**99.2**	**99.9**	**99.5**	**99.4**	**99.5**	**99.6**	**99.5**	**100.0**	**98.1**	**98.8**	**98.4**	**98.0**
Si	1.934	1.952	1.932	1.884	1.887	1.872	1.872	1.873	1.854	1.809	1.676	1.884	1.997	1.973	1.995
Al^{IV}	0.076	0.048	0.068	0.116	0.113	0.128	0.128	0.127	0.146	0.191	0.324	0.110	0.003	0.027	0.005
Al^{VI}	0.006	0.027	0.018	0.041	0.063	0.062	0.066	0.079	0.081	0.113	0.118	0.100	0.074	0.060	0.059
Ti	0.010	0.011	0.011	0.025	0.028	0.033	0.037	0.038	0.042	0.059	0.117	0.029	0.012	0.010	0.010
Fe	0.523	0.536	0.541	0.571	0.584	0.555	0.513	0.525	0.557	0.639	0.653	0.824	0.565	0.512	0.518
Mg	1.316	1.244	1.246	1.061	0.923	0.859	0.814	0.742	0.677	0.543	0.496	0.781	1.197	1.284	1.286
Ca	0.104	0.134	0.147	0.262	0.343	0.430	0.495	0.542	0.582	0.594	0.572	0.262	0.119	0.098	0.095
Na	0.002	0.0	0.0	0.0	0.001	0.000	0.004	0.003	0.002	0.002	0.004	0.002	0.0	0.002	0.0
Cr	0.030	0.032	0.034	0.035	0.038	0.042	0.044	0.041	0.034	0.022	0.020	0.008	0.032	0.034	0.031

CHEMISTRY: A few analyses have been published (Table 2) but not including rare-earth data. There has been little specific discussion of the 15499 composition, other than to note that the sample is in the quartz-normative basalt group. Gibson et al. (1975) presented data for CO, CO_2, H_2, H_2S, and Fe^0, and Kaplan et al. (1976) also presented an Fe^0 abundance.

STABLE ISOTOPES: Gibson et al. (1975) reported $\delta^{34}S$ determinations of +0.2 (,20) and -0.9 (,20), and Kaplan et al. (1977) reported sulfur isotopic determinations which are similar, $\delta^{34}S = 1.2$ (from combustion sulfur) and +0.6 (from hydrolysis sulfur).

RADIOGENIC ISOTOPES AND GEOCHRONOLOGY: According to Albee et al. (1972), Huneke, Podosek, and Wasserburg determined a ^{40}Ar-^{39}Ar age of 3.40 b.y. for 15499; this data has not otherwise been published. Husain (1974) found that the $^{40}Ar^*/^{39}Ar^*$ release pattern was somewhat perplexing, but derived an age of 3.34 ± 0.08 b.y. from the 1000°C, 1200°C, and 1400°C releases (Fig. 7). Although tabulated as "no radiogenic Ar loss" the K-Ar age is slightly lower, 3.328 + 0.036 b.y., and Husain (1972) previously reported a small (0.8%) radiogenic argon loss.

Compston et al. (1972) and Papanastassiou et al. (1973) presented whole-rock Rb-Sr isotopic data (Table 3). Compston et al. (1972) found the difference between subsplits to be consistent with dispersion along a 3.3 b.y. isochron. Assuming this age, the initial $^{87}Sr/^{86}Sr$ ratios for two splits would have been 0.69945 and 0.6996 ± 3 (sic).

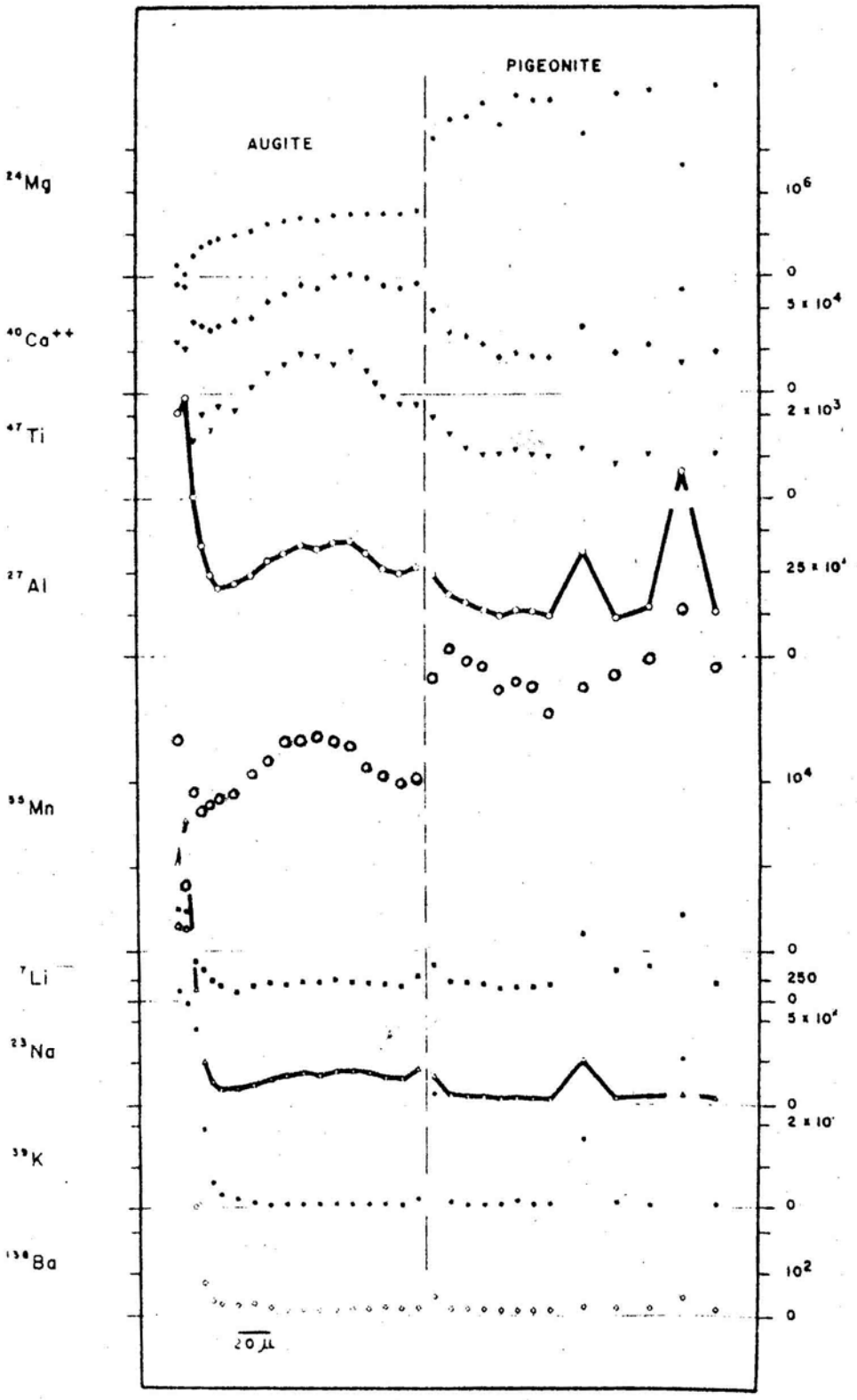

Figure 5. Variation of trace elements across pyroxene in 15499
(Bence and Autier, 1972)

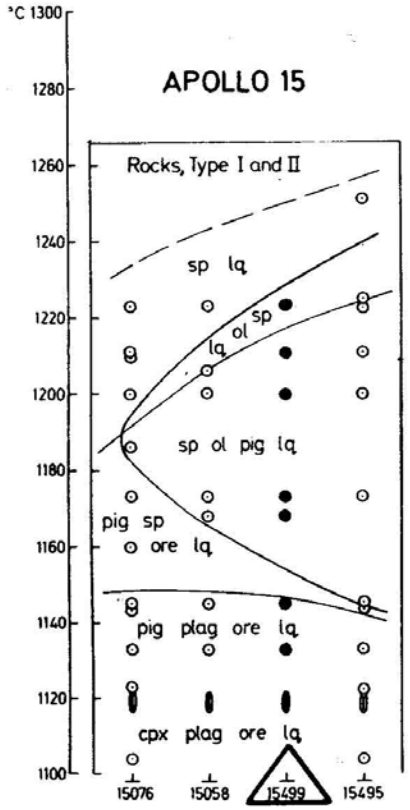

Figure 6. Experimental equilibrium crystallization data for 15499 and other quartz-normative basalts (Humphries et al. al., 1972).

EXPOSURE: Husain (1974) determined an Ar exposure age of 114 m.y. Eldridge et al. (1972) provide cosmogenic radionuclide data; evidently the sample was without much exposed surface area. The equilibrium concentrations of ^{26}Al and ^{22}Na mean that the exposure has been too long to allow an estimate using the $^{26}Al/^{22}Na$ method.

TRACKS: Hutcheon et al. (1972) studied crystals at the bottom of two vugs from the surface of 15499. They observed no micro-craters. The largest crystals were pigeonite prisms without resolvable edge rounding but with a matte finish as if they were rough on a submicroscopic scale. Polished vertical sections were made through the vugs. One vug, ellipsoidal with only a narrow neck to the exterior, had a track density which dropped off very rapidly with depth in the outer few microns of crystals, but the high background track density (~1 x 10^8 cm^{-2}) precluded measuring the gradient at a depth of a few microns. The background was probably accumulated before the rug was exposed, the steep gradient when some chip above the vug was removed. A second vug has a track profile steeper than seen in any other lunar rock or meteorite, >5 x 10^{10} cm^{-2} near surface to ~10^8 cm^{-2} a few tens of microns below (Fig. 8). This profile is as steep as that on the Surveyor spacecraft, and much steeper than on an eroded surface. An exposure time of ~10^5 years was estimated for the vug. Price at el. (1973) discussed this data, noting that the vug interior escaped erosion.

TABLE 15499-2

			,9	,2	,20	,22	,11	,72	,104	,18	,19	,12
Wt %	SiO2	47.89		47.62				47.93				
	TiO2	1.81		1.81				1.73				
	Al2O3	9.19		9.27				8.88				
	FeO	20.47		20.26				19.84				
	MgO	9.11		8.94				9.93				
	CaO	10.41		10.40				10.23				7.3
	Na2O	0.38		0.29				0.29				
	K2O	0.06	0.058	0.06				0.028				0.054
	P2O5	0.08		0.08				0.083				
(ppm)	Sc											
	V							189				
	Cr	3600						4200				
	Mn	2300		2200				2100				
	Co							44				
	Ni							19	51			
	Rb	0.90						1.4	1.2	0.96d	1.08	
	Sr	109.4						100		108.7d	114.3	
	Y	28						31.1				
	Zr	111						109				
	Nb	8						5.4				
	Hf											
	Ba							69				
	Th		0.59									
	U		0.16						0.173			
	Pb											
	La											
	Ce											
	Pr											
	Nd											
	Sm											
	Eu											
	Gd											
	Tb											
	Dy											
	Ho											
	Er											
	Tm											
	Yb											
	Lu											
	Li											
	Be											
	B											
	C				12	27.8b	9.9b	12				
	N							<2				
	S	600a		700		805c	855c	640c	660			
	F											
	Cl											
	Br											
	Cu								3			
	Zn								<2	1.07		
(ppb)	I											
	At											
	Ga	3000										
	Ge									4.28		
	As											
	Se									115		
	Mo											
	Tc											
	Ru											
	Rh											
	Pd									<0.61		
	Ag									0.99		
	Cd									3.37		
	In									0.90		
	Sn									23		
	Sb									1.42		
	Te									3.2		
	Cs									49.1		
	Ta											
	W											
	Re									0.007		
	Os									<0.06		
	Ir									0.0043		
	Pt											
	Au									0.013		
	Hg											
	Tl									0.32		
	Bi									<0.16		
		(1)	(2)	(3)	(4)	(5)	(5)	(6)	(7)	(8)	(9)	(10)	(11)

References to Table 15499-2

References and methods:
(1) Chappell and Green (1973); XRF
(2) O'Kelley et al. (1972); Gamma ray spectroscopy
(3) Rhodes and Hubbard (1973); XRF
(4) Moore et al. (1973)
(5) Gibson et al. (1975); Combustion, hydrolysis
(6) Kaplan et al. (1976)
(7) Duncan et al. (1976); XRF
(8) Wolf et al. (1979); RNAA
(9) Compston et al. (1972); XRF, IDMS
(10) Papanastassiou and Wasserburg (1973)
(11) Busaln (1974); MS

Notes:
(a) quoted as 590 ppm by Gibson et al. (1975) from a Moore 1974 checklist.
(b) from CO, CO_2 abundances.
(c) lower abundances were derived from acid hydrolysis.
(d) average of three determinations.

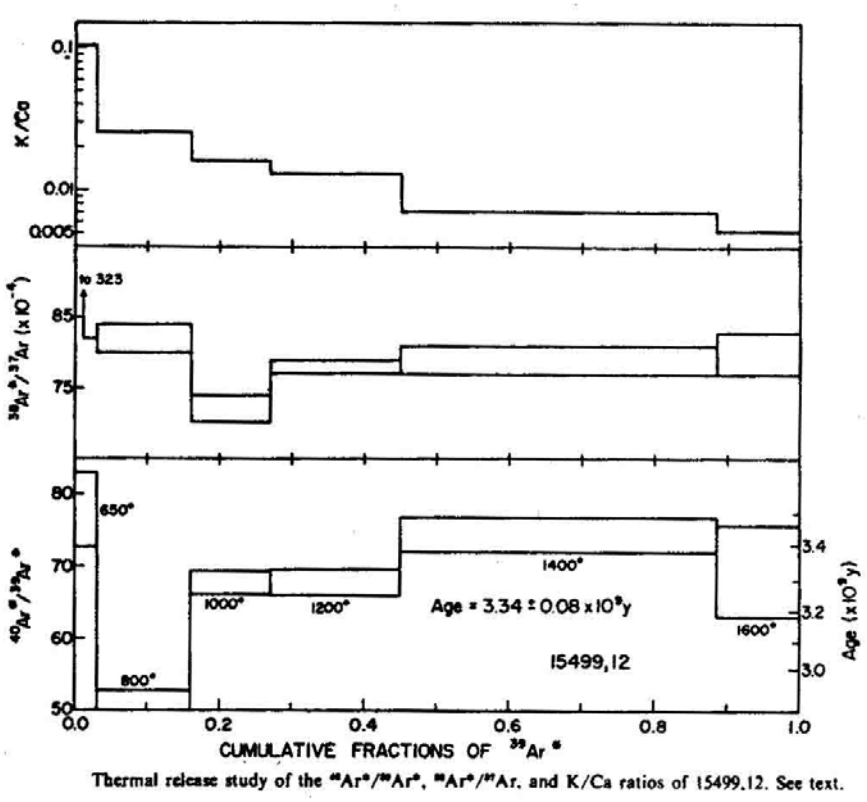

Figure 7. Ar release diagram
(Husain, 1974).

TABLE 15499-3. Rb-Sr isotopic data for 15499 whole rock sample

Reference	$^{87}Rb/^{86}Sr$	$^{87}Sr/^{86}Sr$	T_{BABI}*
Compston et al. (1972)	0.0248	0.70062 ± 10	4.33
Compston et al. (1972)	0.0280	0.70092 ± 25	4.22
Compston et al. (1972)	--	0.70077 ± 10	--
Papanastassiou and Wasserburg (1973)	0.02740 ± 11	0.70064 ± 11	4.28

*from Nyquist (1977)

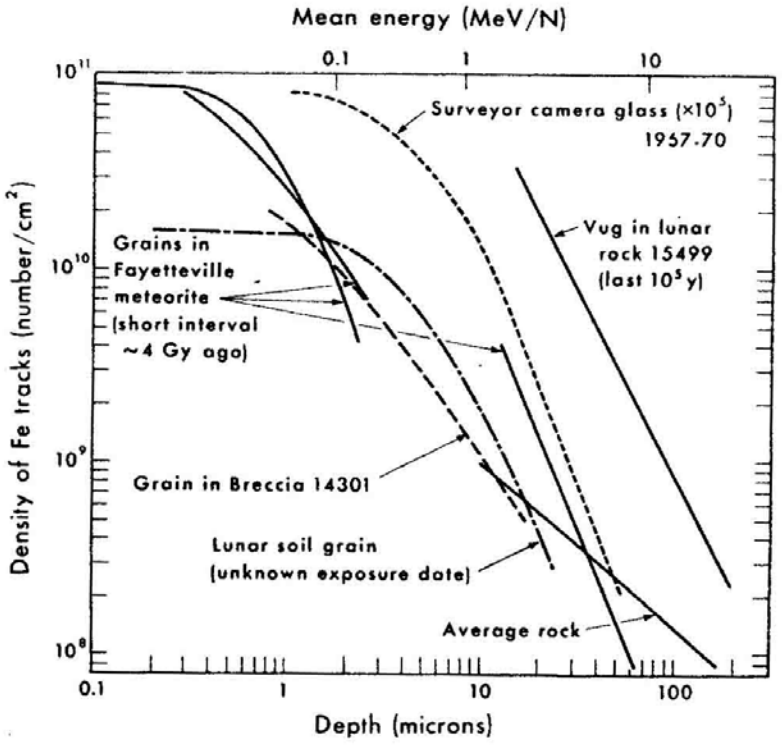

Figure 8. Track density profile of Hutcheon et al. (1972) (from Price et al., 1973).

PHYSICAL PROPERTIES: Collinson et al. (1972, 1973) presented basic magnetic and NRM data (Fig. 9). Split ,21 shows a steady movement of the NRM direction up to the maximum demagnetizing field used of 350 Oe. Split ,27, undergoing stepwise, thermal demagnetization up to 810°C, showed no change in the initial susceptibility at each stage, and this is typical of basalts. The NRM persists up to the Curie point of iron, its apparent carrier. Split ,27 also shows a steady migration of NRM direction up to the iron Curie point, i.e., no stable direction is revealed up to ~750°C. Split ,21 has a low viscosity

coefficient. Artificial thermoremanence gives a TRM proportional to the applied field; an ambient field of 1000 gammas is derived using some assumptions. The results are not easy to interpret in a single magnetization history of a single thermoremanence event in a linear field.

Fuller et al. (1979) also studied the NRM (Fig. 10) finding a large soft component, and a poor directional stability under AF-demagnetization.

Adams and McCord (1972), using diffuse reflectance spectra (0.35 to 2.5 μm) to determine the wavelength positions of the two crystal-field absorption bands contributed by pyroxene, found 15499 to be one of the most augitic Apollo 15 rocks. Charette and Adams (1975) presented spectral reflectance data on a powdered sample: the vitrophyric texture produces a shallower 0.5 to 0.75 μm slope than coarser rocks.

PROCESSING AND SUBDIVISIONS: 15499 was broken into three large pieces ,0; ,9; and ,10 (the only sawing was on ,26). Only a few pieces were taken from ,0 (now 1128 g). ,9 was totally subdivided, with the two largest pieces being ,67 (177 g) and ,76 (377 g); the latter is in remote storage. The largest remaining piece of ,10 became a PAO display (163 g). A chip ,1 was made into thin sections ,4 to ,8, and two pieces of ,10 were made into potted butts ,14 and ,25, producing thin sections ,40; ,42; ,62; ,95; and ,43 and ,44 respectively.

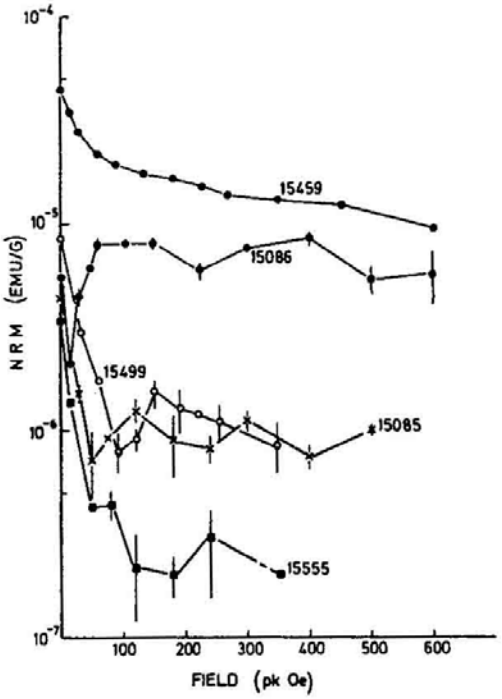

Alternating field demagnetization of Apollo 15 samples. Vertical bars indicate range of intensities obtained after repeated demagnetization.

Figure 9. Magnetic data (Collinson et al., 1973).

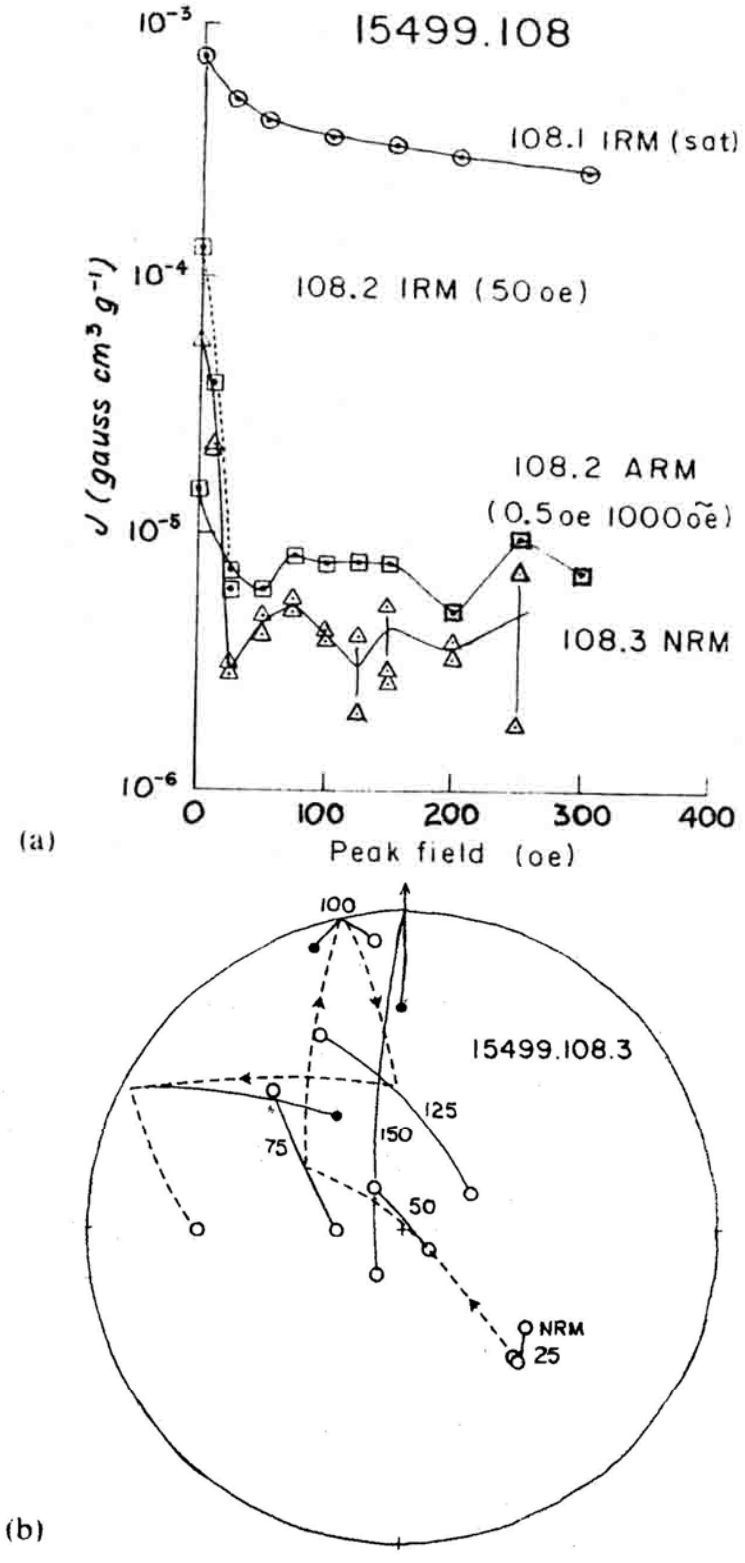

AF demagnetization characteristics of 15499,108.
a) intensity changes, b) directional changes

Figure 10. Magnetic data (Fuller et al., 1979).

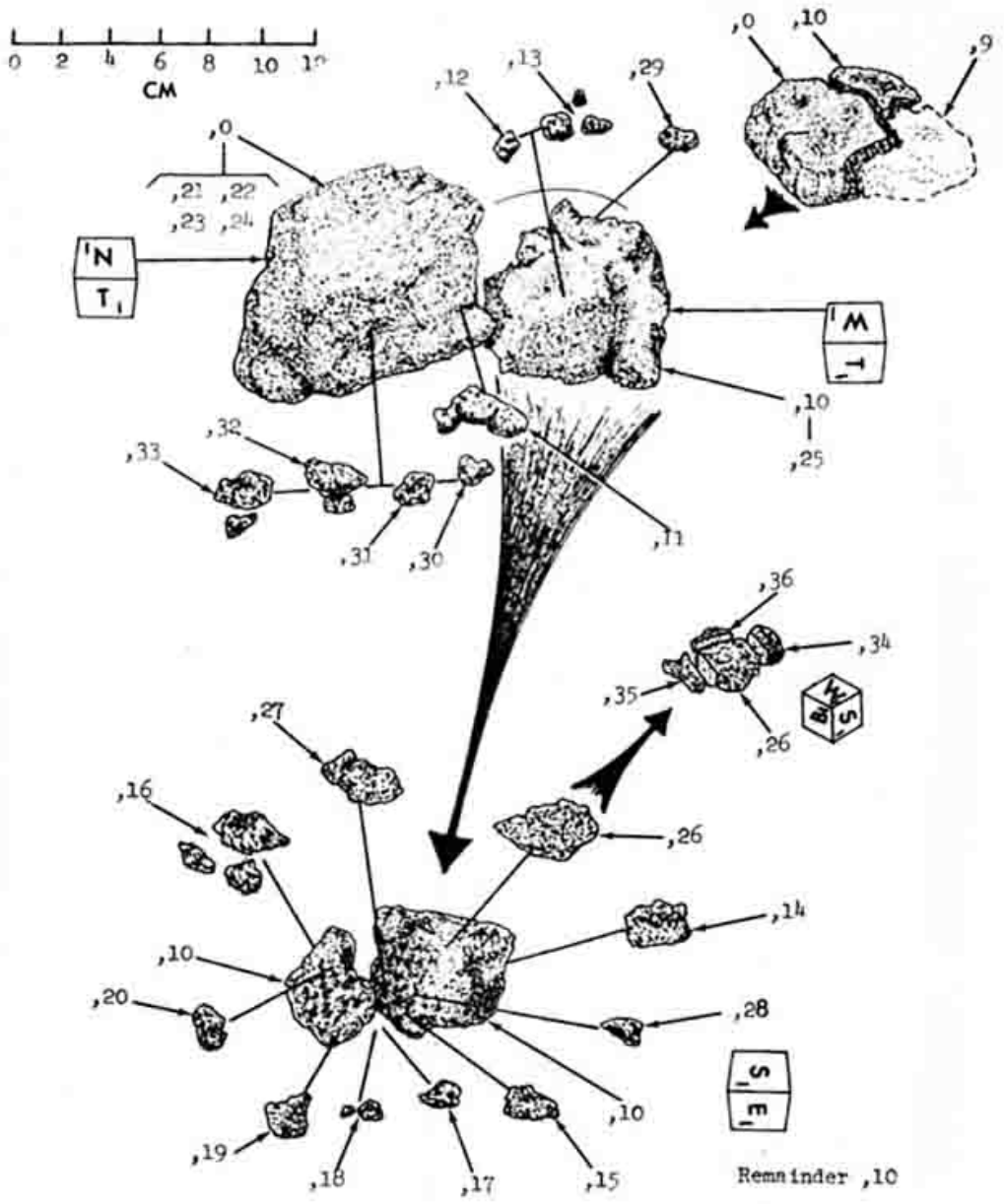

Figure 11. Dissection of 15499.